Reprinted from *J. Mol. Biol.* (1981) **146**, 101–117

Conformational and Geometrical Properties of β-Sheets in Proteins

I. Parallel β-Sheets

F. R. Salemme and D. W. Weatherford

J. Mol. Biol. (1981) **146**, 101–117

Conformational and Geometrical Properties of β-Sheets in Proteins

I. Parallel β-Sheets

F. R. SALEMME AND D. W. WEATHERFORD

Department of Biochemistry
New Chemistry Building
University of Arizona, Tucson, Ariz. 85721, U.S.A.

(Received 9 October 1979, and in revised form 17 September 1980)

The present work treats the geometry of idealized, twisted parallel β-sheets and compares their local and long-range conformational properties to structures known from protein crystallography. Idealized model structures were generated by a least-squares search procedure designed to maximize interchain hydrogen-bond interactions between polypeptide chains of standard geometry whose degrees of freedom were restricted to systematic variations in the backbone torsional angles ϕ and ψ. Two continuously defined sets of regular, twisted, double-stranded conformations, corresponding to structures composed of either straight-helical or coiled-coil polypeptide chains, were investigated both with respect to quality of interchain hydrogen bonding and extensibility into multiply stranded structures. In either case, the introduction of increasing twist into the structure is accompanied by some degree of hydrogen bond distortion that ultimately restricts the extent of twist that may be accommodated in the sheet.

The long-range geometrical configurations of twisted sheets are shown to primarily reflect an equilibrium between the forces that cause the individual polypeptide chains to twist in order to minimize their local conformational potential energies, and the requirements for interchain hydrogen bonding, which generally tend to resist the introduction of twist into the sheet. These effects manifest themselves differently, depending on the adjacent chain hydrogen-bonded connectivity in the sheet, and so account for the differences in the spatial configurations attained by rectangular plan sheets and β-barrel forming, rhombic plan sheets.

Comparison of observed β-structures with idealized model structures shows that, to the extent that the observed structures are regularly hydrogen bonded, they are closely approximated by the models, average α-carbon superposition errors between model and observed structures for the cases examined typically being less than 0·8 Å.

This is the first in a series of three papers describing the structural properties of β-sheets in proteins.

1. Introduction

The flat β-pleated sheet conformations of polypeptides were first described by Pauling & Corey (1951). Although subsequent crystallographic investigations have shown β-sheets to be common secondary structural features of globular proteins,

0022-2836/81/050101-17 $02.00/0

the observed β-sheet conformations differ from the originally proposed flat model structures in that they are almost invariably twisted in a right-handed sense when viewed along the polypeptide chain direction (Chothia, 1973). The observed chiral behaviour is consistent with the results of conformational energy studies on extended polypeptides composed of L-amino acids, which show that their most stable conformations have slight left-handed helical character (Ramachandran, 1974). Owing to the alternating pattern of the hydrogen-bonding interactions in β-sheets, this local left-handed effect endows the chains of extended sheets with an overall right-handed apparent twist (e.g. see Fig. 4 of Weatherford & Salemme, 1979).

The objectives of the work described here were to establish the conformational behavior of idealized, twisted β-sheets that maintain reasonable interchain hydrogen-bonding, and to compare this idealized behavior with representative β-structures observed in protein crystallographic studies. The present approach to the problem of how a flat β-sheet might spontaneously deform in response to the tendency of its individual chains to twist was developed from a consideration of the basic mechanical and symmetry properties of these structures. To begin with, it is evident that flat β-sheets are regular periodic arrays of internally symmetric (i.e. 2-fold helical) polypeptide chains that are interconnected by hydrogen bonds. These structures can consequently be viewed as essentially two-dimensional crystal lattices in which the individual atoms are mechanically interconnected, either by covalent bonds along the direction of the polypeptide chains or by the hydrogen bonds between the chains. Since it is known from conformational energy studies that the localized effects responsible for polypeptide chain twisting are of small magnitude (i.e. typically a few tenths of a kcal/mol per residue (Ramachandran, 1974)), it is apparent that the twisting of a β-sheet along a lowest energy deformation pathway will involve alterations in those internal degrees of structural freedom that are governed by comparably low-energy and slowly varying potential functions. In a β-sheet, these are clearly the backbone torsional angles ϕ and ψ (Ramachandran, 1974), and the low energy deformation modes of the hydrogen bond (Hagler *et al.*, 1974). Further, since the internal degrees of freedom within the structure are governed by such soft potential functions, the most stable conformation of a twisted sheet will generally be that which simultaneously minimizes and most uniformly distributes any stresses accompanying twisting throughout the entire structure. As a consequence, it is to be expected that in the absence of external perturbing effects, the most stable sheet configurations will be those best preserving the interaction equivalence between structural subunits (e.g. peptide groups or single chains), and so retain the highest overall symmetry consistent with the requirements of interchain hydrogen bonding. As shown here, these basically mechanical properties of β-sheets suffice to explain many features of their local and long-range geometry.

2. Methods

The computational approach used in this study has been described (Weatherford & Salemme, 1979). Basically, the procedure involves the generation of duplicate deca-alanine co-ordinate sets of standard geometry (Ramachandran *et al.*, 1974) containing additional

"phantom" atoms corresponding to the expected positions of the carbonyl oxygen, the amide nitrogen, and the amide hydrogen atoms of hypothetical adjacent chains, assuming straight (N–H . . . O) hydrogen bonds 2·8 Å in length. Various twisted sheet structures were subsequently generated by the variation of the deca-alanine polypeptide backbone torsional angles ϕ and ψ in 2° steps, followed by least-squares rotation to find the optimal superposition between the real and phantom atoms involved in interchain hydrogen bonds. The resulting structures were compared quantitatively by computation of the mean difference between the actual and expected (phantom) positions of the N, H and O atoms in the 2 chains. From the preceding search procedure it was possible to define a unique and continuous set of progressively more twisted structures having minimally distorted interchain hydrogen bonds. The computationally obtained behaviour was checked qualitatively using mechanical models having essentially the same degrees of freedom as those assumed in the computational models (Salemme, 1978).

The objective of this computational approach was to produce twisted structures that maintained optimal hydrogen-bond geometry. For the reasons outlined in the Introduction, the optimum hydrogen-bond geometry for the parallel sheet was considered to be that which was both consistent with the maintenance of the symmetry of the flat structure and corresponded to the established isoenergetic deformation modes of the hydrogen bond. As described by Hagler *et al.* (1974), the isoenergetic deformation modes of the N–H . . . O–C hydrogen bond are those which (1) maintain near constancy of the hydrogen bond length, (2) retain colinearity between the N–H and N–O hydrogen bond vectors, but (3) allow the bond to bend at the peptide carbonyl oxygen. Since the interchain hydrogen-bonded interactions in β-structures must generally lie in the plane of the sheet, it was additionally assumed that deformations involving bending at the carbonyl oxygen were restricted to arrangements in which the linear NHO bond vector remained in the plane of the carbonyl oxygen sp^2 orbital (i.e. the plane defined by Cα, C, N and O). This latter restriction is suggested by the observations that random deviations in hydrogen-bond geometry that cause them to project out of the sheet plane must necessarily result in longer than optimal interchain hydrogen bonds in extended structures, whereas systematic deformations result in sheets that are bent along an axis midway between the polypeptide chains, so giving rise to non-equivalent and/or sterically unacceptable Cβ contacts on opposite sides of the sheet. According to these foregoing constraints, it is readily demonstrated that owing to the symmetry properties of parallel sheets, their optimal interchain hydrogen-bonding geometry is linear (see Results). Consequently, this feature was incorporated into the phantom hydrogen-bonding atoms of subsequently generated *parallel* twisted sheets. As shown in the following paper, *antiparallel* sheets differ from parallel sheets in that the optimal interchain hydrogen bonding geometry of the former arrangement is not constrained to be linear.

Co-ordinates for model structures of extended β-sheets used for comparison with observed protein structures were generated by least-squares rotation of appropriate substructures (e.g. single strands or coiled-coil double-strand structures) to obtain the best superposition of atoms involved in interchain hydrogen bonding.

Protein co-ordinate data were obtained from the Brookhaven Protein Data Bank (Bernstein *et al.*, 1977) and the Atlas of Macromolecular Structure on Microfiche (Feldman, 1976). Several structures from this atlas are reproduced or referred to here, and are designated by S (Sheet) or B (Barrel), followed by fiche number, row and column. Reference to this source will provide specific residue numbering and inclusive references to the respective structure determinations.

3. Results

(a) *Conformational properties of regular parallel structures*

(i) *A unique flat structure*

Figure 1 shows a flat, double-stranded parallel β-sheet having standard geometry

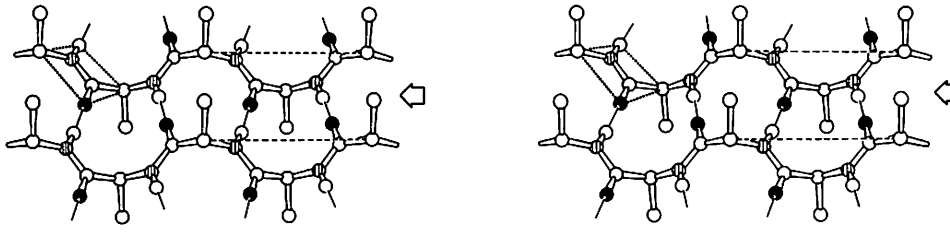

FIG. 1. A section of flat, double-stranded, parallel β-sheet: 2-fold screw symmetry axes relate successive residues of each chain. An additional 2-fold screw axis located midway between the 2 chains relates each pair of residues forming a hydrogen-bonded ring with those preceding or following it. The local interchain twist is here defined as the angle between vectors of adjacent chains (broken lines) from ith to $(i+2)$nd α-carbon atoms. The backbone torsional angles for the flat structure with 2·8 Å (N–H . . . O) hydrogen bonds are $\phi = -116°$, $\psi = 112°$. Nitrogen atoms are shaded, oxygen atoms are black. The broad arrow indicates the N to C chain direction.

and 2·8 Å (N–H . . . O) hydrogen bonds. The structure is composed of straight chains whose residues are related by successive 180° rotations and unit translations (i.e. 2-fold screw symmetry operations) along the axis of each polypeptide backbone chain. Such 2-fold helical structures are, in general, characterized by the set of ϕ, ψ values that define the flat helical ($n = 2$) line on the ϕ, ψ plot (Fig. 2). The structure having straight interchain hydrogen bonds between parallel-running chains occurs at a single point on the $n = 2$ line at $\phi = -116$, $\psi = 112°$.

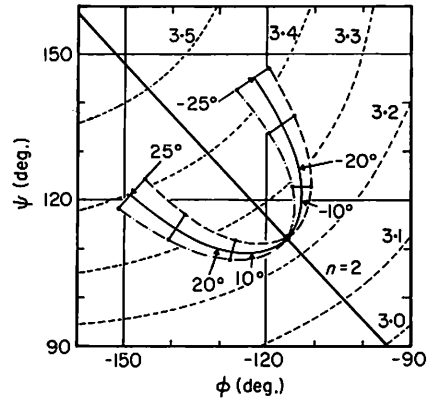

FIG. 2. A ϕ, ψ plot showing the computed conformational pathways for the twisting of parallel β-sheets. The flat structure lies on the $n = 2$ helix line at $\phi = -116°$, $\psi = 112°$. Right-twisted sheets are composed of chains that are locally left-handed helices, and so lie to the right of the $n = 2$ line. Crossing interactions made between straight helical chains are characterized by a single ϕ, ψ value for all residues of each progressively more twisted structure. These conformations form a continuous set, which describes the unbroken curve on the plot. Double-stranded, coiled-coil structures are characterized by a continuous set of sequentially alternating pairs of ϕ, ψ values, shown schematically as connected points between the long-dashed curves on the plot. Degree quantities give local interchain twist as defined in Fig. 1. Short-dashed lines show the variation in d, the rise along the helix axis per peptide unit in straight helical chains, as a function of ϕ and ψ. Both the crossing and coiled-coil conformations become more extended relative to the flat structure as they are progressively twisted. The slightly asymmetrical behavior of the rise lines (d) about the $n = 2$ line arises from the fact that the $C\alpha(i)-C'$ and $C\alpha(i+1)-N$ vectors of the amide peptide bond are not exactly coparallel. As a result, the geometrical properties of right- and left-twisted structures differ slightly, although this effect is minimal in the region of the ϕ, ψ plot corresponding to extended polypeptide chain conformations.

When viewed in plan, each hydrogen-bonded ring in this structure forms a trapezoid whose inclined sides correspond to the linear interchain hydrogen bonds, and whose parallel sides correspond to the mean axes of the polypeptide chains. If the chain conformations are modified to obtain alternative flat helical conformations (i.e. the ϕ, ψ values of the best hydrogen-bonded flat structure are varied up or down the $n = 2$ line), this changes the repeat period of the chains and causes the projected angle between each chain's hydrogen-bond groups, and the mean chain axes to vary. As a result, the inclined sides of the projected trapezoids no longer meet, which is to say, that the N–H and N–O vectors of the hydrogen bonds do not remain colinear. Since this is an energetically unfavorable deformation of a hydrogen bond (Hagler *et al.*, 1974), it is clear that the $\phi = -116°$, $\psi = 112°$ flat structure with straight hydrogen bonds is a unique structure, which has optimal interchain hydrogen bonds.

(ii) *Regular twisted structures*

There are two ways in which the flat structure may be systematically deformed to produce regular twisted structures (Weatherford & Salemme, 1979). In what follows, we first consider how an isolated, double-strand parallel sheet twists to produce double-helical coiled-coiled structures. As shown, this arrangement is geometrically incompatible with the formation of multiply stranded sheets, whose geometrical properties are consequently best approximated by straight helical chain crossing structures.

(iii) *Coiled-coil parallel structures*

Figure 1 shows a short section of flat, double-strand parallel β-sheet. If the polypeptide chains of this structure are to twist in response to the minimization of the backbone ϕ, ψ torsional potentials, it is evident that twisting the asymmetric ring formed by any two residues of the adjacent chains, while preserving the associated interchain hydrogen bonds, will induce different ϕ, ψ rotations at the α-carbons on opposite sides of the ring. This results in the formation of a twisted structure whose polypeptide chains are coiled-coils, and whose regularly repeating subunit is a dipeptide that is conformationally characterized by a pair of ϕ, ψ values. Owing to the restrictions arising from interchain hydrogen-bond periodicity and directionality, there exists a unique and continuously defined set of progressively more twisted coiled-coil, double-strand structures that are associated with the optimal preservation of the interchain hydrogen bonding (Fig. 2). The ϕ, ψ values describing the local conformation of these structures alternate for successive residues along the polypeptide chains and across the hydrogen-bonded rings of the sheet. It is relevant to point out here that there are, in principal, a large number of local conformational configurations (i.e. sets of ϕ, ψ values) that will produce coiled-coil structures of similar overall geometry (Nishikawa & Scheraga, 1976), but that the requirements for optimal interchain hydrogen bonding between chains restricts this set to the specific conformations lying along the lines shown in Figure 2.

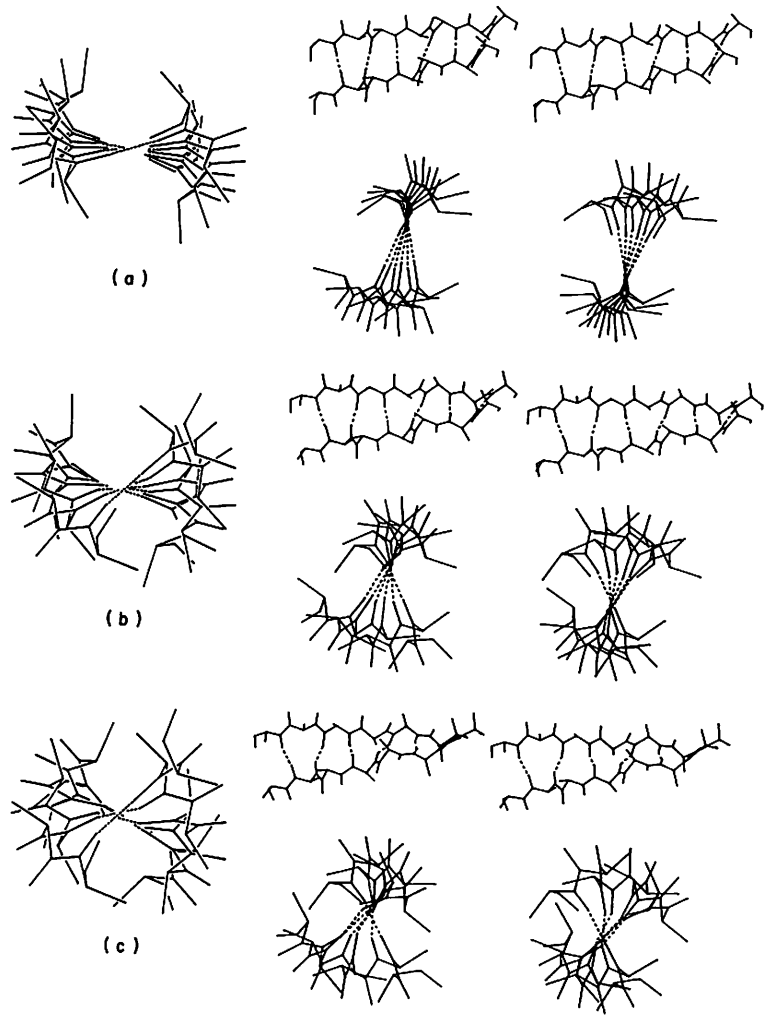

FIG. 3. Double-stranded, parallel, coiled-coil structures with chains of 7 residues and 6 hydrogen bonds. As can be seen from both the stereoscopic and projection end views, parallel coiled-coils form symmetrical double-helical structures of approximately constant overall radius. (a) Structure with $\phi_1 = -112°$, $\psi_1 = 120°$, $\phi_2 = -116°$, $\psi_2 = 120°$; average NHO bond length 2·82 Å, standard deviation 0·04 Å, local interchain twist $= -10·4°$. (b) Structure with $\phi_1 = 109°$, $\psi_1 = 128°$, $\phi_2 = -119°$, $\psi_2 = 128°$; average NHO bond length $= 2·82$ Å, standard deviation 0·16 Å, local interchain twist $= -16·6°$. (c) Structure with $\phi_1 = -112°$, $\psi_1 = 136°$, $\phi_2 = -124°$, $\psi_2 = 140°$; average NHO bond length = 2·82 Å, standard deviation 0·36 Å, local interchain twist $= -18·0°$.

Figure 3 shows views of three representative right-twisted, coiled-coil structures. The polypeptide chains of these structures conform to a centrally located superhelix axis that approximately intersects the interchain hydrogen bonds, so that the chains of all possible parallel coiled-coil structures conform to a cylindrical surface of constant superhelical radius R, where $2R = D$, the mean interchain separation. Double-helical coiled-coils having small interchain twists are essentially infinitely extensible along the polypeptide chain direction. For larger twists, the

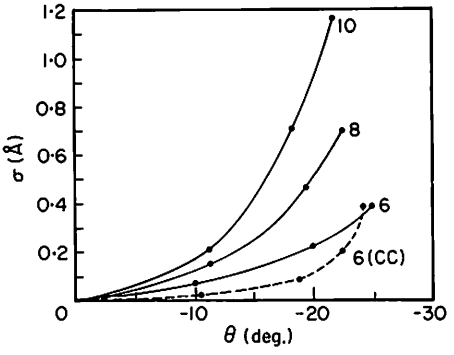

FIG. 4. Hydrogen-bonding characteristics of twisted parallel β-sheets. The least-squares procedure described in Methods produces structures in which the average hydrogen bond length is 2·8 ± 0·1 Å. The plot shows the standard deviation in hydrogen bond length (σ) in crossing structures with 6 (5 hydrogen bonds), 8 (7), and 10 (9) residues in adjacent strands, as a function of interchain twist (θ) as defined in Fig. 1. Structures having fewer interchain hydrogen bonds can accommodate a greater extent of interchain twist concomitant with any fixed value of hydrogen bond distortion. The broken curve (6(CC)) shows the behavior of a double-strand (6 residues/strand) coiled-coil. The hydrogen-bond distortion of this structure is less than for an equivalently twisted crossing structure for small to moderate interchain twist angles, but rises rapidly for larger interchain twists. This behavior gives some indication of the extent to which the coiled-coil structure may be twisted about its superhelix axis while preserving the interchain hydrogen bonds.

hydrogen bonds of coiled-coils become more distorted. This situation arises owing to the constant radius characteristic of the twisted parallel coiled-coils, which requires that the polypeptide chains traverse a progressively larger distance on the cylindrical surface defined by the chain supercoil as the structure is twisted. As a result, the polypeptide chains are required to simultaneously become more coiled and more extended, a situation that is conformationally incompatible with maintenance of the interchain hydrogen bonds. The rather abrupt onset of serious hydrogen-bond distortion with increasing interchain twist is shown in Figure 4 for a six-residue by two-strand coiled-coil. In longer structures, the onset of serious hydrogen-bond distortion occurs at smaller values of interchain twist, suggesting that these structures become less torsionally flexible as they are lengthened. As pointed out in a survey by Richardson (1977), isolated double-strand parallel structures are rarely found in proteins of known structure. Instead, parallel β-sheets are almost invariably observed to form multiple-strand structures. As shown in Figure 5, multiple-strand β-sheets of rectangular plan cannot be built up of extensively twisted coiled-coil chains, since this would require any central strand to simultaneously conform to two local superhelical axes. The only way in which this situation may be approximated is if the coiled-coil chains have such small twists that their conformations are practically indistinguishable from straight helical chains (e.g. see Weatherford & Salemme, 1979).

(iv) *Crossing parallel structures*

In Figure 2 are shown the computed curves for the twisting of a parallel β-sheet in which all ϕ, ψ values are constrained to be identical, so giving rise to structures

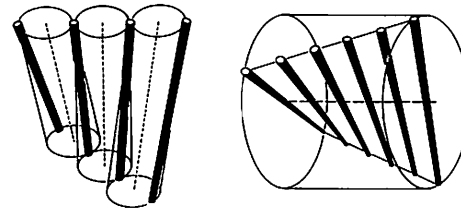

FIG. 5. (a) A schematic illustration of the geometrical properties of a β-sheet of rectangular plan, composed of polypeptide chains of coiled-coil conformation. In order for any central chain to conform to 2 local helical axes (broken lines), the chains must be essentially straight helices related by small interchain twist angles. Such structures lie close to the flat structure on the ϕ, ψ plot (Fig. 2), and so are virtually indistinguishable from those composed of straight-helical chains (b).

composed of straight helical polypeptide chains. As shown, there again exists a well-defined pathway in ϕ, ψ space that is uniquely associated with the optimal preservation of the interchain hydrogen bonding. However, as shown in Figure 4, the twisting of a structure composed of straight helical chains is accompanied by the introduction of rather more cumulative distortion in the interchain hydrogen bonding relative to similarly twisted coiled-coil structures of moderate twist. This is an obvious consequence of the reduction of the number of independent conformational degrees of freedom in the crossing *versus* coiled-coil conformations. It is apparent that the straight helical chains of crossing structures must eventually diverge in space, so that the extent of good interchain hydrogen bonding that may be attained is inversely related to both the chain length and the degree of interchain twist (Fig. 4). The structural relevance of such crossing interactions stems from the fact that they may be infinitely extended along the direction of the hydrogen bonds to produce multiply stranded structures in which the interactions between a strand and each of its neighbors are identical. Although the finite twisted sheets that occur in globular proteins would reasonably be expected to manifest a continuum of conformations, in which central sheet chains most closely resemble crossing conformations and edge chains take on coiled-coil conformational character, such structures may practically be approximated as hydrogen-bonded arrays of straight helical crossing chains. This approximation holds principally, because similarly twisted crossing and coiled-coil conformations do not differ significantly in their local conformational properties (Fig. 2). Indeed, it is evident that in the limit of an infinitely extended sheet, both conformations must converge on the common flat structure.

Figure 6 shows a representative, multiply stranded right-twisted parallel β-sheet that was generated by the successive least-squares hydrogen-bond superposition of straight helical chains of identical conformation. The structure that results is consequently that which minimizes the extent of cumulative hydrogen-bond deformation between adjacent strands. Although the hydrogen bonds of this structure are slightly deformed, it is evident from the equivalence of the interchain twist and the overall regularity of the structure, that the least-squares minimization procedure has uniformly and symmetrically distributed these

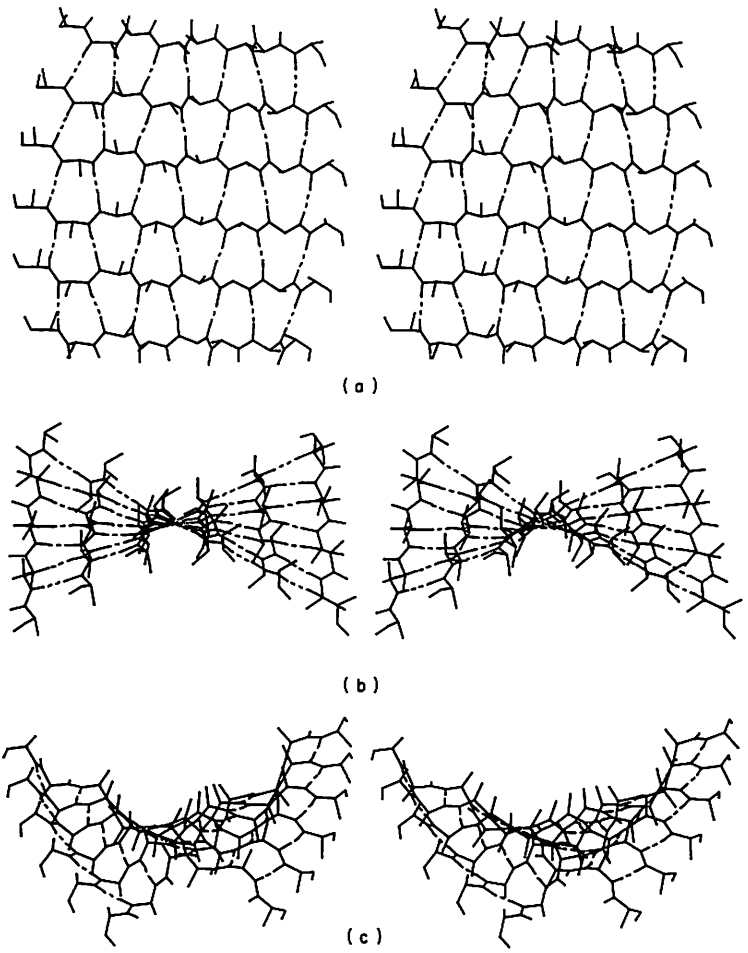

FIG. 6. Views of a multiply stranded, right-twisted parallel β-sheet composed of crossing, straight helical polypeptide chains ($\phi = -114°$, $\psi = 122°$). Although each strand makes identical interactions with its neighbors, the hydrogen bonds in the center of each chain are necessarily shorter than those at the ends and overall somewhat distorted (e.g. see Weatherford & Salemme, 1979). Since the chains of such structures must eventually diverge, structures having fewer interchain hydrogen bonds can accommodate larger overall interchain twists for a given average value of hydrogen bond distortion. For the structure shown, the interchain twist is $-14{\cdot}0°$, the average hydrogen bond (NHO) length is 2·82 Å, with a standard deviation of 0·24 Å. Note that the constant rate of interchain twist in such rectangular plan structures results from both local conformational effects governing directionality of the interchain hydrogen bonds and the change in peptide repeat period of the structure as it is twisted (Fig. 2). (a) View normal to sheet. (b) View down central chains of sheet. (c) Skew view showing sheet curvature.

distortions throughout the structure as a whole. In order to test how well the spatial configurations of the observed structures corresponded to the idealized behavior predicted from the model studies, two observed rectangular plan parallel sheets were modeled as perfectly regular crossing structures. We emphasize that the only variable parameter utilized in this fitting procedure was the single ϕ, ψ value common to all residues of the crossing model structure, which was

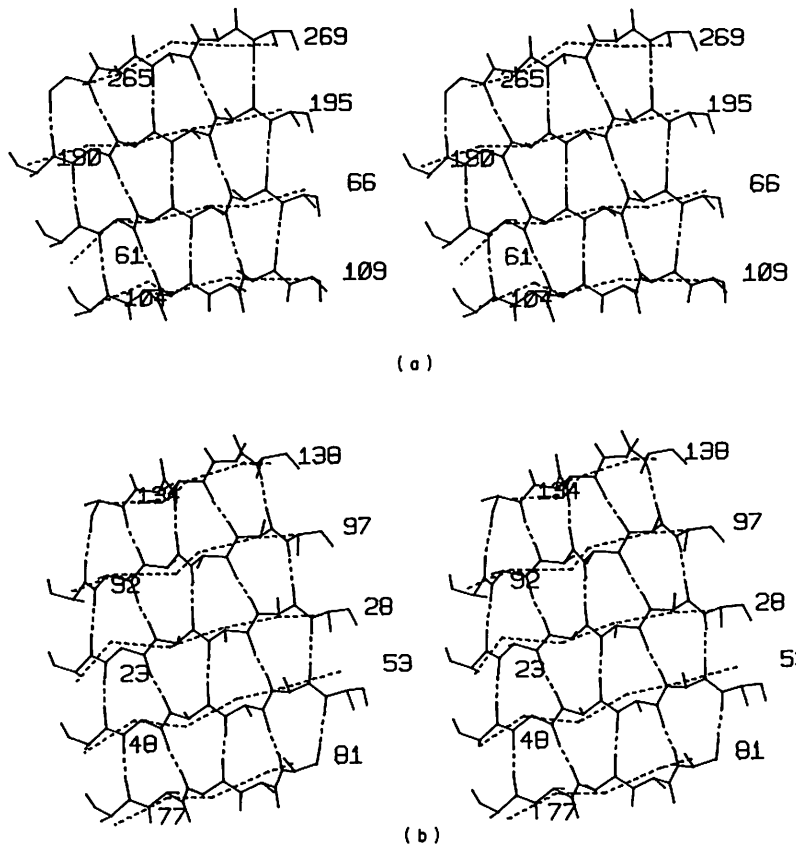

FIG. 7. (a) Stereo view of a crossing model structure ($\phi = -114°$, $\psi = 120°$, average NHO bond length 2·82 Å, standard deviation 0·08 Å, interchain twist $= -12·8°$) superimposed on the 4 central parallel strands (residues 61 to 66, 104 to 109, 190 to 195, 265 to 269) of the carboxypeptidase β-sheet (broken lines). The average α-carbon superposition error is 0·75 Å.

(b) Stereo view of a crossing model structure ($\phi = -114°$, $\psi = 124°$, interchain twist = 117·6°, average NHO bond length 2·83 Å, standard deviation 0·15 Å) superimposed on residues 23 to 28, 48 to 53, 92 to 97, 134 to 138 and 77 to 81, of the lactate dehydrogenase β-sheet (broken lines). The average superposition error of α-carbons is 0·77 Å.

constrained owing to the requirements of optimal interchain hydrogen bonding to lie along the corresponding curve shown in Figure 2. Extended model structures were subsequently generated by least-squares superposition of the interchain hydrogen bonds exactly as described above (Fig. 6).

Figure 7(b) shows a least-squares superposition of a regular twisted parallel model structure with the five-strand β-sheet in lactate dehydrogenase (Chandrasekhar *et al.*, 1973). The mean superposition error for the 28 α-carbon atoms common to the structures is 0·77 Å. Figure 7(a) shows a crossing model *versus* observed structural fit for the central four parallel strands of the eight-strand mixed β-sheet in carboxypeptidase A (Quicho & Lipscomb, 1971). The mean superposition error for the 23 C_α atoms common to the two structures is 0·75 Å. Although both structures conform reasonably well to model crossing structures

with respect to the constancy of interchain twist and resulting overall geometry, these similarly connected sheets have differing rates of twist (Fig. 7). This is contrary to expectation since, other factors being equal, the degree of twist should be governed by the extent of concomitant hydrogen-bond distortions. The larger rate of interchain twist in the lactate dehydrogenase structure may be related to the fact that it is an isolated sheet that is unconstrained by any requirements for regular hydrogen bonding at its edges. The carboxypeptidase parallel sheet, in contrast, is located in the center of a larger mixed sheet whose outer-strand hydrogen-bonded interactions may geometrically restrict the extent of local distortion possible in the inner parallel strands. Equivalently, variation in the twist of these sheets may also reflect the existence of co-operative effects that impart increased stabilization to the hydrogen bonds that occur in extended networks (Sheridan *et al.*, 1979). This effect could confer additional stability to the more extended across-the-sheet hydrogen-bond interactions in the carboxypeptidase structure relative to the lactate dehydrogenase sheet, and consequently make the former structure more resistant to the introduction of hydrogen-bonding distortions that accompany twisting.

(v) *Rhombic-plan sheets and β-barrels*

Some parallel β-sheets in proteins have approximately rhombic plans resulting from a staggered hydrogen-bonding arrangement of adjacent chains. These staggered arrangements form structures of approximately cylindrical symmetry, the well-known β-barrels (Richardson, 1977). Figure 8 shows a typical structure generated by least-squares hydrogen-bond superposition (see Methods) of straight helical chains in a staggered array. In the structure that results, each polypeptide makes closest approach interchain interactions with adjacent chains that differ in position along the central chain. As a consequence of this systematic interchain rise and twist, the structure as a whole takes on apparent cylindrical symmetry.

(vi) *Closure requirements for eight-strand parallel barrels*

The structure shown in Figure 8 is clearly only one of many such cylindrically symmetric structures that may be differentiated according to polypeptide interchain twist, and the number and arrangement of interchain hydrogen bonds. The structures of immediate relevance to proteins are those of eight-strands that close to form regular cyclically hydrogen-bonded cylinders. As is evident from Figure 8, both the accessible cylindrical radii of curvature and the pitch angle of chains on the cylindrical barrel surface are correlated variables ultimately dependent on the local interchain hydrogen-bonded interactions. Figure 9 shows a closed eight-strand cylinder in which there are three hydrogen bonds between adjacent chains. In order to generate this structure it was necessary to (1) utilize chain conformations that lie considerably off the curve shown in Figure 2 and (2) introduce a somewhat irregular stagger pattern between adjacent chains of the structure. As is implicit in Figure 4, the adjustment of the crossing polypeptide chain conformations to obtain a structure whose twist produces the required cylindrical pitch and curvature has a relatively small effect on the quality of the

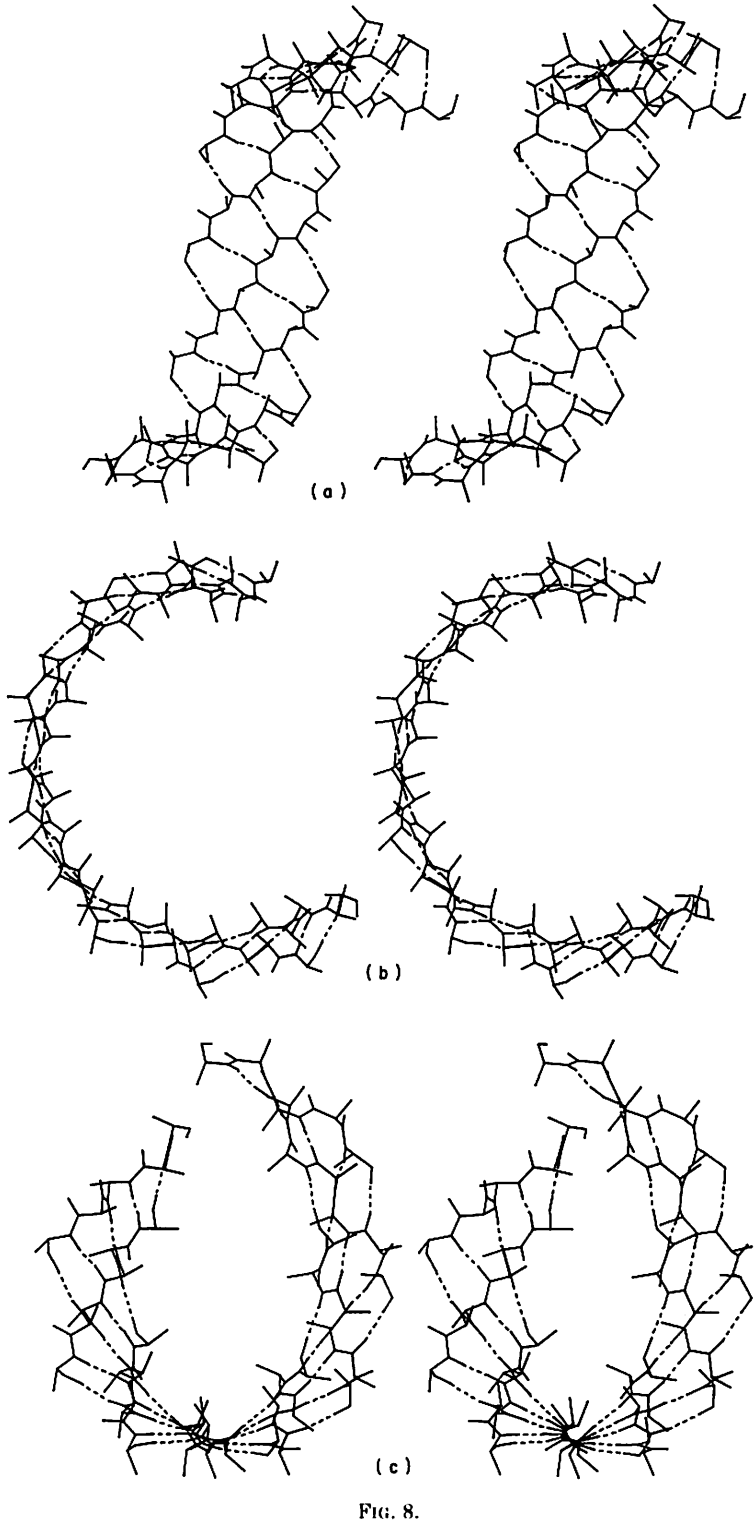

FIG. 8.

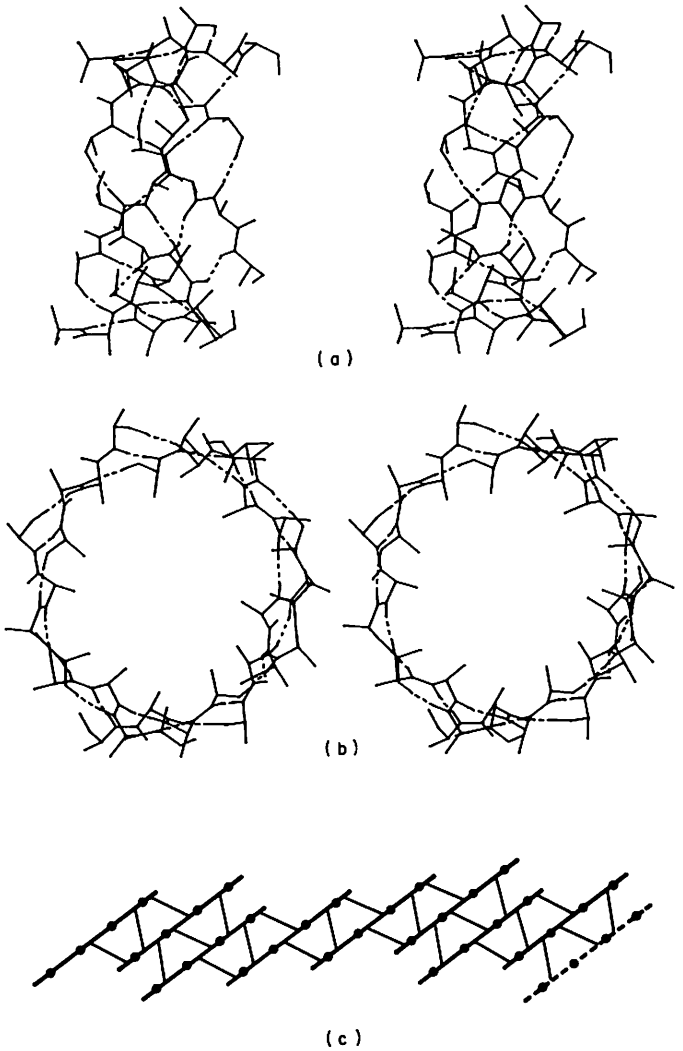

FIG. 9. A model 8-strand parallel β-barrel composed of straight helical chains ($\phi = -102{\cdot}5°$, $\psi = 129°$). The pattern of adjacent chain stagger is dissimilar in different regions of this structure, although each strand makes 3 hydrogen bonds with its neighbors. (a) Side view. (b) View down the cylinder axis. The diameter of this cylinder is approximately 16 Å. Mean hydrogen bond length = 2·76 Å, standard deviation = 0·18 Å, local interchain twist = −33°. (c) Hydrogen bond plan.

FIG. 8. An 8-strand rhombic sheet composed of identical crossing chains ($\phi = -114°$, $\psi = 128°$, interchain twist = −20°C, average hydrogen bond length = 2·83 Å, standard deviation = 0·21 Å). There are 6 residues in each chain, 5 hydrogen bonds between any 2 adjacent chains and 3 hydrogen bonds across any 3 adjacent chains. The structure as a whole has a right-handed wrap about the defining cylinder axis. (a) Side view. (b) View slightly skew from cylinder axis showing the elliptical curvature of the structure. (c) View down a single chain axis.

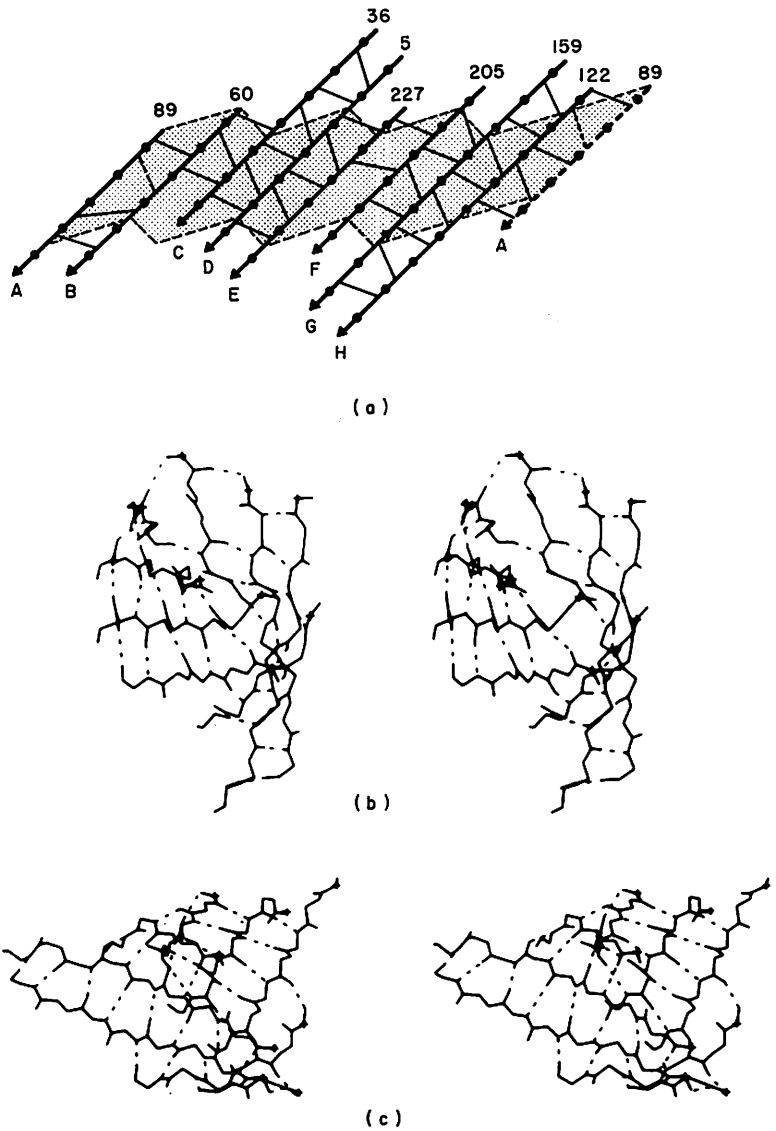

FIG. 10. The triose phosphate isomerase β-barrel. (a) Schematic hydrogen bond plan. The shaded overlay shows the adjacent chain stagger pattern of the 8-strand model structure shown in Fig. 9. (b) AMSOM B2K16; (c) AMSOM B311; (see Feldman, 1976).

interchain hydrogen bonds. In other words, the distribution of conformations for polypeptide chains required to make only three local hydrogen-bonded interactions of a specified quality is significantly broader than for interactions involving larger numbers of hydrogen bonds. Attempts at modeling regular, cyclically hydrogen-bonded barrel structures with four or more adjacent hydrogen bonds failed to produce structures that both close and have interchain hydrogen bonds that are neither excessively long nor distorted.

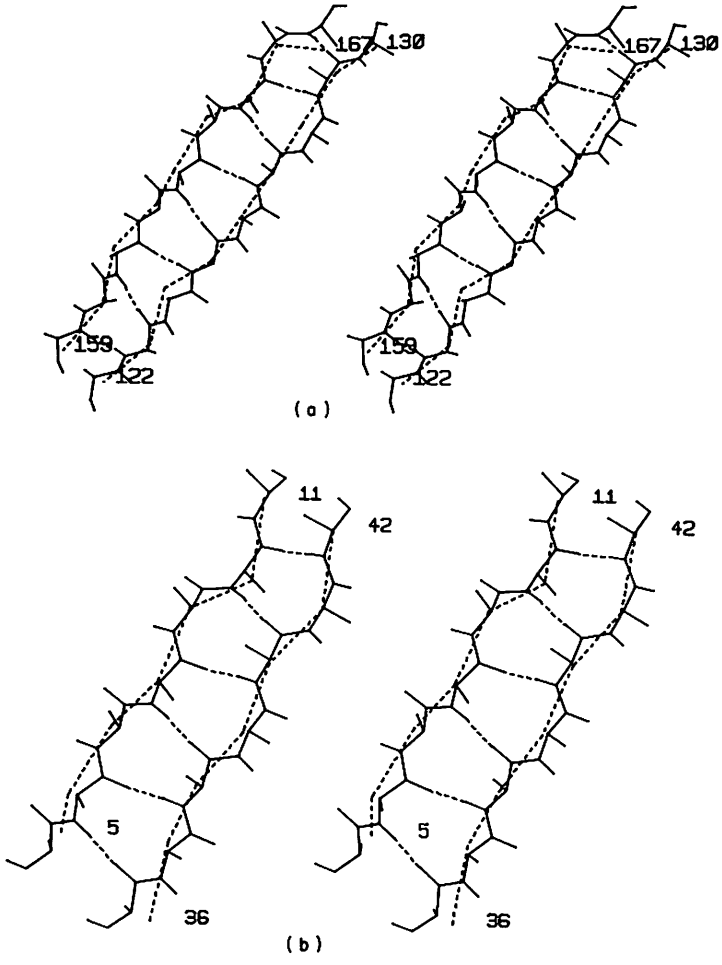

FIG. 11. Least-squares fits of model coiled-coil structures (unbroken lines) onto substructures of the observed (broken lines) triose phosphate isomerase structure. (a) Coiled-coil with $\phi_1 = -112°$, $\psi_1 = 124°$, $\phi_2 = -116°$, $\psi_2 = 128°$, average NHO bond length = 2·83 Å, standard deviation = 0·17 Å, fit to strands G and H (Fig. 10(a)) with an average α-carbon superposition error of 0·69 Å. (b) Coiled-coil with $\phi_1 = -116°$, $\psi_1 = -112°$, $\phi_2 = -112°$, $\psi_2 = 122°$, average NHO bond length = 2·77 Å, standard deviation = 0·07 Å, fit to strands C and D with an average α-carbon superposition error of 0·50 Å.

(vii) *The parallel β-barrel in triose phosphate isomerase*

Figure 10 shows a schematic hydrogen-bond plan and stereoscopic views of the eight-strand (Monomer-1) β-barrel of triose phosphate isomerase (Banner *et al.*, 1975). The shaded overlay on the hydrogen-bond plan shows the similarity in the overall stagger pattern between the model (Fig. 11) and observed barrels; otherwise, the structures differ both in their local and long-range properties. Instead of being cylindrically symmetrical, the observed structure is, in contrast, organized into regions having extended, regular hydrogen bonding: a triple-strand structure (CDE) and a quadruple-strand structure (FGHA). As a result of the

extended along-the-chain hydrogen bonding in these substructures, their local cylindrical radii of curvature are larger than those of the barrel as a whole. Closure of the structure therefore necessitates strongly twisted interactions and irregular hydrogen-bond formation between strands A and B and strands E and F, to give a barrel whose cross-section is more elliptical than circular. Attempts at modeling the substructures indicate that the two longest contiguously interacting strands of each region (CD and GH) are best approximated by model coiled-coils (Fig. 11), whose ϕ, ψ values differ slightly from those determined for the best hydrogen-bonded *isolated* double-strand structures described in Figures 2 and 3. As a consequence, the hydrogen bonds of these model substructures are more distorted than those of the isolated double-strand structure, as can be seen from comparison of the data in Figures 4 and 11. The observed arrangement apparently maximizes the extent of curvature that may be locally accommodated in the substructures at the expense of the regularity in conformation of the adjacent strands and the hydrogen bonds that these strands in turn make with their neighbors. The overall conformation of the structure appears to be dominated by the requirements of side-chain close-packing in the interior of the barrel (Richards, 1977), which may be attained only at the expense of the local hydrogen bond integrity.

4. Conclusion

The similarity in the spatial configurations of parallel β-sheets among otherwise structurally disparate proteins is an observation of long standing (Rossmann & Argos, 1976; Rossmann & Liljas, 1974; Rao & Rossmann, 1973). Here it has been shown that the spatial arrangement of parallel β-sheets in proteins can, to a good approximation, be described as arising from local conformational constraints associated with the maintenance of periodic interchain hydrogen bonding when the structures are twisted. Since the extent of twist that may be introduced into β-sheets is, in large part, determined by the number and arrangement of adjacent chain hydrogen bonds, it is to be expected that β-sheets of similar plan will have qualitatively similar tertiary conformations.

This research was supported by grants from the National Institutes of Health (GM21534 and GM25664), the University of Arizona Computer Center, and a Dreyfus Teacher-Scholar Grant (to F.R.S.).

REFERENCES

Banner, D. W., Bloomer, A. C., Petsko, G. A., Phillips, D. C., Pogson, C. I., Wilson, I. A., Corran, P. H., Furth, A. J., Milman, J. D., Offord, R. E., Priddle, J. D. & Waley, S. G. (1975). *Nature (London)*, **255**, 609–614.

Bernstein, F. C., Koetzle, T. F., Williams, G. J. B., Meyer, E. F. Jr, Brice, M. D., Rodgers, J. R., Kennard, O., Shimanouchi, T. & Tasumi, M. (1977). *J. Mol. Biol.* **112**, 535–542.

Chandrasekhar, K., McPherson, A., Adams, M. J. & Rossmann, M. G. (1973). *J. Mol. Biol.* **76**, 503–528.

Chothia, C. (1973). *J. Mol. Biol.* **75**, 295–302.

Feldman, R. J. (1976). *Atlas of Macromolecular Structure on Microfiche*, Tractor-Jitco, Rockville.

Hagler, A. T., Lifson, S. & Huler, E. (1974). In *Peptides, Polypeptides and Proteins* (Blout, E. R., Bovey, F. A., Goodman, M. & Lotan, N., eds), pp. 35–48, Wiley Interscience, New York.
Nishikawa, K. & Scheraga, H. (1976). *Macromolecules*, **9**, 395–401.
Pauling, L. & Corey, R. B. (1951). *Proc. Nat. Acad. Sci., U.S.A.* **37**, 729–740.
Quicho, F. A. & Lipscomb, W. N. (1971). *Advan. Protein Chem.* **25**, 1–78.
Ramachandran, G. N. (1974). In *Peptides, Polypeptides and Proteins* (Blout, E. R., Bovey, F. A., Goodman, M. & Lotan, N., eds), pp. 14–34, Wiley Interscience, New York.
Ramachandran, G. N., Kolaskar, A. S., Ramakrishnan, D. & Sasisekharan, V. (1974). *Biochim. Biophys. Acta*, **359**, 298–302.
Rao, S. T. & Rossmann, M. G. (1973). *J. Mol. Biol.* **76**, 241–256.
Richards, F. M. (1977). *Annu. Rev. Biophys. Bioeng.* **6**, 151–176.
Richardson, J. S. (1977). *Nature (London)*, **268**, 495–500.
Rossmann, M. G. & Argos, P. (1976). *J. Mol. Biol.* **105**, 75–95.
Rossmann, M. G. & Liljas, A. (1974). *J. Mol. Biol.* **85**, 177–181.
Salemme, F. R. (1978). *J. Mol. Biol.* **126**, 591–595.
Sheridan, R. P., Lee, R. H., Peters, N. & Allen, L. C. (1979). *Biopolymers*, **18**, 2451–2458.
Weatherford, D. W. & Salemme, F. R. (1979). *Proc. Nat. Acad. Sci., U.S.A.* **76**, 19–23.